

## **Efficiency Improvement of a tidal current turbine utilizing a larger area of channel**

Ki-Pyoung Kim<sup>a</sup>, M. Rafiuddin Ahmed<sup>b</sup> and Young-Ho Lee<sup>c\*</sup>

<sup>a</sup>Maritime R & D Centre, Korean Register of Shipping, Daejeon, Korea

<sup>b</sup>Division of Mechanical Engineering, The University of the South Pacific, Suva, Fiji

<sup>c</sup>Division of Mechanical and Energy Systems Engineering, Korea Maritime University, Busan, Korea

Corresponding author: Prof. Young-Ho LEE

Division of Mechanical and Energy Systems Engineering  
Korea Maritime University, 1 Dongsam-dong Youngdo-ku,  
Busan, 606-791, Republic of Korea

Tel: +82-51-410-4293, Fax: +82-51-403-0381

Mobile: +82-10-3862-4293

E-mail: lyh@hhu.ac.kr

# Efficiency Improvement of a tidal current turbine utilizing a larger area of channel

Ki-Pyoung Kim<sup>a</sup>, M. Rafiuddin Ahmed<sup>b</sup> and Young-Ho Lee<sup>c\*</sup>

<sup>a</sup>*Maritime R & D Centre, Korean Register of Shipping, Daejeon, Korea*

<sup>b</sup>*Division of Mechanical Engineering, The University of the South Pacific, Suva, Fiji*

<sup>c</sup>*Division of Mechanical and Energy Systems Engineering, Korea Maritime University, Busan, Korea*

*\*Email: lyh@hhu.ac.kr*

## Abstract

There is a growing interest in utilizing tidal currents for power generation which has led to extensive research on this source of renewable energy. The amount of energy that can be extracted from tidal currents has been a topic of considerable interest to researchers for many years; still, there is no consensus on the extent to which this resource can be exploited. A turbine generates no power if it presents no resistance to the flow or if it presents so much resistance that there is no flow through it. At the same time, the estimation of exploitable resource should take into consideration the environmental, economic and social constraints. In view of these, the design of efficient turbines driven by bi-directional tidal currents has been a challenge to researchers for some time. There appears to be a general agreement among researchers that a number of turbines spread over the width of the channel can extract more energy compared to an isolated turbine. The present work is aimed at quantifying the improvement in the performance of a given type of turbine by utilizing a larger area of the channel. Numerical experiments were performed using the commercial CFD code ANSYS-CFX to study the performance of a bi-directional cross-flow turbine by simulating two cases of i) a single turbine and ii) a number of equally spaced turbines. It was found that the Coefficient of Power can be increased significantly by employing a larger area of the channel.

*Keywords:* Ocean energy; Tidal current; Cross-flow turbine; CFD; Coefficient of power

## Nomenclature

A	inlet area of augmentation channel, $m^2$
$C_p$	Power Coefficient
H <sub>l</sub>	length of augmentation channel from inlet to the axis of the turbine, m
P	rotor Power, W
P <sub>o</sub>	power output of turbine, W
P <sub>w</sub>	water power upstream of a given turbine, W
R	blade radius, m
TSR	tip speed ratio
V <sub>l</sub>	height of augmentation channel at inlet, m
V <sub>aci</sub>	mean velocity at augmentation channel inlet, m/s
V <sub>ri</sub>	mean velocity at rotor inlet, m/s
$\rho$	density of sea water, $kg/m^3$
$\Omega$	angular velocity, rad/s
U <sub>o</sub>	freestream velocity, m/s

## 1. Introduction

Many countries surrounded by the oceans have rich marine energy resources, hence significant amount of electric power can be generated from the oceans. Marine currents offer a regular and predictable source of renewable energy [1]. Marine currents have only recently been looked at seriously for large-scale power generation. A marine current turbine utilizes the kinetic energy of marine currents and converts it to mechanical energy. Researchers have tried unsuccessfully to employ conventional hydro-turbines for extracting energy from marine currents, because the available head is too small. The main difference between high-head and free flow turbines is that that the latter need large flow openings to capture as much water mass as possible with low velocities and pressure. Conventional turbines, in contrast, are designed for high pressure and relatively small water ducts where all the water is made to pass through the turbine. These turbines have efficiencies as high as 90%. This is simply not possible for free flow turbines. Even the Betz limit of 59.3% is considered unachievable [2] especially by propeller-type turbines because the assumption in the Betz model is that the fluid flow remains rectilinear when passing

through the turbine and maintains a uniform distribution of its pressure on the turbine. Such a uniformly distributed load leads to an overestimation of the force acting on the turbine and, as a result, an overestimation of the turbine's output and efficiency. In reality, the fluid streams are deflected from the rectilinear direction near the barrier, changing their motion to curvilinear trajectories and reducing their pressure on the turbine [2].

A tidal current turbine has to extract energy from the bi-directional flow of water. There is a growing interest in utilizing tidal currents for power generation and as a result, a surge in research efforts directed at this renewable energy resource [3-11]. Garrett and Cummins [3] did a theoretical analysis of an isolated turbine and an array of turbines in a channel. A turbine generates no power if it presents no resistance to the flow or if it presents so much resistance that there is no flow through it. They opined that an isolated turbine will inevitably have a current through it with a speed lower than the ambient current, with a consequent reduction in power generation below the metric of  $0.5\rho U_o^3$  per unit cross-section. They also concluded that an array of turbines in the entrance to a bay plant will be most effective if it is spread across the width of the entrance in order to minimize free flow past the turbines. They also felt that too many turbines may choke the flow and reduce the power. Atwater and Lawrence [4] also did a theoretical analysis to estimate the power generation potential in a channel. They argued that it is inappropriate to use the free kinetic energy flux as the available resource because it does not account for the reduction in flow as a result of increased resistance. For the determination of the ideal turbine resistance, they suggested that a relation between friction and velocity needs to be established; normally, the variation in the head loss with velocity is linear to quadratic. If the relationship is quadratic, a maximum of 38% of the fluid power of a channel may be extracted, and if the relationship is linear, the maximum drops to 25%. They also concluded that the flow will reduce to 57% for the quadratic case and 50% for the linear case. Bryden and Couch [5] studied the possible energy extraction from a simplified channel model and concluded that the undisturbed kinetic flux density is a useful indicator of achievable resource. They suggested that if higher levels of flow alteration are acceptable, then substantial fraction (called Significant Impact Factor) of the energy may be available for extraction. In another paper, Garrett and Cummins [6] performed a theoretical analysis for the cases of an isolated turbine and a tidal fence occupying different fractions of a channel cross-section. They concluded that the

maximum efficiency factor  $16/27$  for a turbine in an infinite medium is increased in a channel. They also concluded that the actual, rather than fractional power will increase if the ratio of turbine area to channel area is increased. Sutherland et al. [7] found that at maximum power extraction, the volume flux drops to 58% of that in the natural state and  $2/3$  of the original head along the whole channel gets transferred to the turbine array. Blunden and Bahaj [8] performed a review of the current understanding of tidal energy resources. The exploitable tidal current resources and some analytical models of energy extraction were reviewed. They questioned the lower achievable efficiency suggested by Gorban et al. [2] in view of the fact that some full-scale prototype tidal current turbines achieved a power coefficient of 0.4 and above.

Sun et al. [9] suggested that estimation of the exploitable resource should not only take into consideration the environmental, economic and social constraints, but also the hydrodynamic resilience of the site in question and the fact that different technologies may give different returns, depending on the nature of the site and the appropriateness of the technology. Their CFD work focused on the impact of tidal current energy extraction on the local flow conditions. Their model simulated the operational conditions for tidal energy extraction, where the flow is constrained in the channel. A wake region is formed behind the tidal energy converter, which is characterized by reduced velocity due to energy loss. Since the mean velocity in the wake is lower than the free-stream velocity, the velocity outside the wake in a closed channel must be higher than the free stream in order to maintain continuity of volume flow rate. Because of this blockage effect, the flow is accelerated around the tidal current turbine. Their CFD results demonstrated that the interaction of the tidal turbine with the flow is a complicated 3D problem. The distortion of the free water surface will distort the wake and further influence the performance of the turbine [9]. Kirke [10] in a research paper opined that the marine current energy conversion technology still requires lot of research because it differs considerably from the wind turbine technology. Significant amount of power can be obtained from tidal currents and the researchers are still investigating different types of turbines and till now, none has emerged as a clear winner. He reviewed some of the turbines that were being evaluated. It was also felt by him and Blunden and Bahaj [8] that the ducted turbine, that was not found to be economically advantageous for wind energy extraction, may be an attractive option for tidal

current energy extraction. Kirke [10] obtained a higher power coefficient,  $C_p$ , for the ducted turbine compared to the open one.

Bahaj et al. [11] performed power and thrust measurements of horizontal axis marine current turbines in a cavitation tunnel and a towing tank and studied the effects of tip speed ratio, the blade pitch angle, blade tip immersion and yawed inflow. The rotor diameter was 800 mm and had higher blockage ratio in the cavitation tunnel compared to the test tank. Since the blades for such a turbine generate rotation mainly by lift, tip speed ratio (TSR) values of 5-7 resulted in optimum performance. Under yawed conditions, the turbine power reduced significantly. In another work on horizontal axis tidal current turbines, Coiro et al. [12] obtained the maximum efficiency at TSR values of 3-4.

Another type of turbine that is attracting considerable attention nowadays is the cross-flow turbine. This type of turbine is suitable even for very small heads. It is essentially an impulse turbine. It can handle large quantities of water and also possesses flat efficiency characteristics. In this type of turbine, the water passes over the blades twice, resulting in a higher momentum transfer [13]. Some of the other advantages of a cross-flow turbine include cost effectiveness, ease of construction, no problem of cavitation and independence of its efficiency to variations in the flow rate [14,15]. Olgun [15] found a very small change in the maximum efficiency of their cross-flow turbine when the head was changed from 8 m to 30 m.

## **2. Cross-flow turbine and the augmentation channel**

The cross-flow turbine studied in the present work consisted of a rotor made up of 26 equidistant blades. An augmentation channel consisting of a nozzle at the inlet side and a diffuser at the exit side surrounded the rotor, as shown in Fig. 1. The flow through the turbine is radial and the water passes over the blades twice before exiting the rotor and entering the diffuser. This is a bi-directional turbine and the design ensures equal output and efficiency for both the directions of the flow. Due to this unique nature of flow - with the flow passage converging during the first pass and diverging during the second pass through the blades and a non-uniform distribution of flow in different blades, it is never desired to run the rotor full as the rotational force is not obtained by reaction as is the case with Francis turbine. Some more of the characteristics of the cross-flow turbine are: i) a wide range of rotational speeds can be selected, ii) turbine diameter

does not depend on the flow rate, iii) efficiency levels are satisfactory, iv) manufacturing is simple and construction can be done at local facilities, and v) the bearings do not come in contact with the flow [15]. Cross-flow turbines have been successfully designed and tested for ocean energy extraction both experimentally and numerically and some of the works have been published [16-18].

The augmentation channel in the present work was designed to generate power bi-directionally without the use of additional devices. In all our related works, the turbine and augmentation channel designs were similar to the present one; however, the shape of the augmentation channel was modified based on the anticipated flow conditions as well as independent research [14]. In the present work, since the source is tidal current, the channel shape shown in Fig. 1 was employed.

In this research work, a cross-flow turbine which is suitable for low-speed and high flow rate is designed and analyzed. Unlike most water turbines, the water passes through the rotor blades transversely in a cross-flow turbine. As with a waterwheel, after passing the rotor, it leaves on the opposite side. Therefore, the water strikes the blades twice, once at the inlet blades and second at the exit blades, thus providing additional energy to the turbine and hence a higher efficiency. The water enters the runner at the specific angle and transfers some of its kinetic energy to the blades. The nozzle before the rotor causes acceleration of the flow and thus the water enters the rotor with increased kinetic energy. The diffuser after the rotor increases the pressure at the expense of the kinetic energy. After exiting the augmentation channel, the flow mixes with the flow that passes around the augmentation channel which is normally at a higher velocity than the freestream velocity. The resulting velocity gradient creates a shear layer with high turbulence levels, which causes rapid mixing of the two flows.

### **3. Design procedure**

The numerical experiments were performed in a water channel having a length of 87 m and a cross-section of 26.1 m x 26.1 m. The design freestream velocity was chosen as 2.5 m/s in this work. The inlet flow was assumed to be uniform across the height and width of the water channel. The inlet area of the augmentation channel (A) is 8.7 m × 8.7 m and the total length is

17.4 m. At the inlet to the turbine, the augmentation channel height reduces to 4.35 m. The internal and external diameters of the rotor are 3.85 m and 6.05 m respectively. The 3D CAD tool used was CATIA [19]. Twenty six blades were provided between the inner and outer periphery of the rotor. The blades make an angle of  $30^\circ$  with the tangent to the rotor at the outer periphery and a right angle with the tangent to the rotor at the inner periphery. Each of the blades has an axial length of 8.7 m, a radial length of 1.1196 m and a thickness of 66 mm. The augmentation channel, which served as a nozzle at the inlet side and as a diffuser at the exit side, is shown in Fig. 2. It was modeled in two halves and placed on either side of the turbine. The curved surface of the augmentation channel was designed to be tangential to the blade at both the inlet and outlet sides. The clearance of the turbine and housing was 20.6 mm. The geometric details of the rotor and the augmentation channel are shown in Table 1. The flatter edge of the augmentation channel was curved near the turbine inlet to ensure smooth entry of the flow to the blades. The direction of the flow entering the rotor is controlled by the shape of the nozzle, indicating the importance of the nozzle shape. The complete blades are shown in Fig. 3.

#### **4. Grid generation**

The commercial code ANSYS-Icem CFD was used for mesh generation. To get a higher accuracy, hexahedral grids were generated. About 1 million nodes were provided on the augmentation channel. The meshed augmentation channel is shown in Fig. 4. It was found easier to generate the grids on one blade and then rotate the whole mesh by  $360^\circ$ . About 200,000 nodes were provided on each blade; hence the total number of nodes on all the blades was about 5.2 million. Figure 5 shows the meshed rotor. In the water tunnel, the number of nodes was about 2 million. Thus, the total number of nodes in the entire domain exceeded 8 million.

#### **5. Computational procedure**

The finite volume commercial code ANSYS-CFX was used in the present computations. This code was tested for the analysis of a similar turbine [16,17]. A good agreement between numerical and experimental results was observed for the flow characteristics through the augmentation channel and the rotor. The work also involved studying the effect of non-dimensional wall distance  $y^+$  on the turbine performance; it was found that for  $y^+ \leq 50$ , the



accuracy does not get affected [20]. In this study three turbulence models were also ‘tested’ for the analysis of a cross-flow turbine. The  $k-\omega$  SST turbulence model gave good results in the simultaneous analysis of both high and low energy areas in a complicated flow field with relatively low grid dependence. Hence, the  $k-\omega$  SST turbulence model was chosen for turbulence modeling. To perform the present CFD analysis, 8-10 parallel computers were employed. The inlet velocity was set at 2.5 m/s with its direction normal to the water tunnel inlet face. The boundary condition at the outlet was set to zero (atmospheric) pressure. The density of the water was taken as  $1025 \text{ kg/m}^3$ . The boundary conditions for the augmentation channel were set to ‘wall’ (no-slip condition). Figure 6 shows the schematic diagram of the water tunnel and a single turbine and augmentation channel set-up inside the tunnel (case 1). The other case (case 2) of multiple equally spaced turbines was simulated by placing four solid walls, with no slip boundary conditions, around a turbine and augmentation channel set-up at a distance of a quarter of the augmentation channel inlet width/height, which comes to 2.175 m. Thus, the case of multiple turbines (with their augmentation channels) placed side-by-side with a reduced spacing between them and thus occupying a greater area of the channel, was simulated. The freestream velocity was same as the previous case. The angular velocity ( $\Omega$ ) was varied to get different values of TSR. The tip speed ratio was calculated taking the mean velocity at the rotor inlet as the reference velocity due to the uniqueness of this study. The water velocity at the entrance to the augmentation channel ( $V_{aci}$ ), at the entrance to the rotor ( $V_{ri}$ ), the power output and the Coefficient of power ( $C_p$ ) were computed at these values of TSR. The results for both these cases are presented in the following section.

## **6. Results and discussion**

### *6.1. Flow characteristics*

The main focus of the present work was on the performance analysis of the bi-directional cross-flow turbine for the two cases of a single turbine and multiple, equally spaced, turbines. However, as the design of the turbine is unique, the flow characteristics through the nozzle, the rotor and the diffuser were studied in detail for both the cases. For both the cases, the flow was found to accelerate on the sides outside of the augmentation channel due to the resistance to the flow offered by the augmentation channel and the closely-spaced turbine blades, which forces the incompressible flow to divert away from the augmentation channel. The tidal current turbine,

introduced in to the tidal current, is known to reduce the flow to as much as 50% of the flow in the absence of the turbine [4]. However, for this particular area reduction and number of blades, the reduction in velocity is larger. Figure 7 shows the velocity vectors for the flow through the augmentation channel and the rotor blades for case 1. It can be seen that the velocity at the entrance of the augmentation channel is less than 1 m/s. The flow is found to separate on the turbine blades as well as in the diffuser. The flow separation is likely to affect the performance of the turbine significantly. The blades rotate through the fluid generating the viscous forces at the layer near the solid surface and the viscous forces cause flow separation between two blades. The flow separation is influenced by the Reynolds number of the local flow. When the adverse pressure gradient is reasonably strong, the flow next to the wall reverses direction, resulting in a region of backward flow. The reversed flow meets the forward flow at some point at which the fluid near the surface is transported out into the mainstream. As a result, the flow separates from the wall. At lower Reynolds numbers, the reversed flow downstream of the point of separation forms part of a large steady vortex behind the surface. At higher Reynolds numbers, when the flow has boundary layer characteristics, the flow downstream of separation is unsteady and frequently chaotic [21]. The separation is known to increase the drag, particularly pressure drag which is caused by the pressure difference between the front and rear surfaces of an object. For this reason much effort and research has gone into the design of aerodynamic and hydrodynamic surfaces which delay flow separation and keep the local flow attached for as long as possible. It is interesting to observe that the flow separates at the trailing edge of the blades resulting in a region of re-circulating flow in the region. The flow through the diffuser section will get affected by the pressure in the near-wake of the augmentation channel. The velocity vectors for the flow through the augmentation channel and the rotor blades for case 2 are shown in Fig. 8. The velocity at the entrance of the augmentation channel is higher than case 1 and more than 1 m/s. The rotational speed of the turbine was varied in the present work such that TSR values varied from 0.15 to 2.7. Figure 9 shows the variation of the velocity at the entrance to the augmentation channel and the rotor with TSR for the two cases. The freestream velocity is constant at 2.5 m/s for all the cases studied in the present work. It is interesting to note that the velocity at the entrance of the augmentation channel ( $V_{aci}$ ) is considerably reduced compared to the freestream velocity ( $U_o$ ) for both the cases; however, for case 2, the mean velocity is nearly twice compared to case 1, indicating that if more turbines are placed in a channel close to each other, the kinetic

energy available to the turbine will be significantly higher, as the flow is forced to pass through the turbine and not go around the augmentation channel. The velocity inside the nozzle increases further as the flow approaches the rotor blades. It can be seen from Fig. 7 and Fig. 8 that most of the flow enters the blades at the centre of the duct at any instant. For the blades in the first stage (when the flow is passing over the blades for the first time), the acceleration of the flow on the upper surface (suction) and the deceleration on the lower surface (higher pressure) can be seen for both the cases. This shows that some of the power generation takes place due to the pressure difference on the two sides of the blades. The water can be seen to accelerate as it exits the first stage blades and flows across towards the second stage blades. However, there is a region of recirculating flow under the region of accelerated flow. To clearly understand the mode of energy transfer from the water to the blades during the second stage, an enlarged view of the rotor showing the flow interaction with the blades for case 2 was analyzed. This is shown in Fig. 10. It can be seen from this figure that the accelerated flow does not enter the second stage blades tangentially. It strikes the blades at an angle and due to the resulting impulse, a force is exerted on the blades. The water transfers some of its momentum to the blades causing them to rotate. Figure 11 shows the pressure contours in and around the augmentation channel and in the rotor for case 2. The pressure starts to build in front of the augmentation channel as the flow decelerates. However, the pressure starts reducing outside of the augmentation channel as the flow starts accelerating in the free gap between the augmentation channel and the separating wall between two turbines. In the region of minimum area in the gap, a strong suction can be seen. The velocity recorded here was slightly more than twice the freestream velocity. Inside the augmentation channel, the pressure is higher than atmospheric at every point with a higher pressure at the inlet section where the area is maximum. As the area reduces towards the rotor inlet, the velocity increases (Fig. 8) and consequently, the pressure reduces a little. As the flow enters the blades, the flow possesses both high velocity and higher pressure. It should, however, be noted that a direct application of energy balance between the inlet of the augmentation channel and the rotor blades will not be appropriate, as the streamlines are curving and most of the flow is entering only some of the blades. As the water exits the first stage blades and flows towards the second stage blades, it still possesses high pressure and velocity except for the recirculating region where the pressure is below atmospheric. At the exit of the rotor, the

pressure is lower, which starts to increase as the flow moves towards the exit of the augmentation channel (diffuser).

## *6.2. Power output and power coefficient*

Figure 12 shows the power output for the two cases. The maximum power output of 54 kW in case 1, found at a TSR of 0.9 is significantly smaller compared to case 2. The torque for both the cases reduced from its maximum at the lowest TSR to the maximum TSR. However, the torque and hence the power output increased considerably for case 2, where the flow was forced to take place through the augmentation channel and the rotor due to the small gap between one turbine set-up and the other. The maximum power output recorded for this case was slightly above 300 kW at a TSR of nearly 1.3. Accordingly, the Coefficient of power,  $C_p$ , was considerably higher for case 2 for all the tip speed ratios studied in this work, as shown in Fig. 13. Interestingly, the minimum  $C_p$  for case 2 was higher than the maximum  $C_p$  for case 1, highlighting the importance of utilizing a larger area of the channel for higher power extraction. As discussed in the previous section, this resulted in a considerably higher flow of water through the turbine which resulted in a higher power generation. The maximum  $C_p$  recorded for case 2 was 0.51, which is more than 5 times the maximum  $C_p$  for case 1. The reasons for the lower  $C_p$  are the high resistance to the flow offered by the augmentation channel's nozzle and the closely-spaced blades, the flow separation between the turbine blades and in the diffuser. It is felt that the large number of blades and the narrow spacing between the blades adversely affect the smooth flow of water. Therefore, to improve the turbine performance, the number of blades and the clearance should be optimized by studying the effect of these parameters on the flow characteristics to reduce the flow resistance and to control the separation. The non-streamlined shape of casing also influences the whole turbine system flow, therefore the effect of shape should be considered when analyzing the whole turbine system. Although a higher  $C_p$  was obtained for case 2, it is felt that the performance can be improved by designing a nozzle with a slightly larger area at the exit, which will also be helpful when the flow takes place in the opposite direction. Utilizing a large area of a real tidal flow channel may not always be practical as it will affect the local flow conditions that may include undesirable conditions for boats and for marine life. In some cases e.g. when the channel is formed between reefs, the effect on the local flow conditions may be undesirable.

The maximum power output and coefficient were obtained at a TSR of around 1. This shows that the cross-flow turbine behaves more like an impulse turbine rather than a lift-driven turbine as is the case with horizontal axis tidal turbines.

The power available in the water upstream of a given turbine ( $P_w$ ) is given by

$$P_w = \frac{1}{2} \rho A U_o^3 \quad (1)$$

In the present case, the quantity  $P_w$  is fixed as the freestream velocity and the augmentation channel inlet area is fixed. It is seen in the above section that the rotor power output and  $C_p$  increase as more turbines are placed in the water channel. This is compared with the theoretical power generated by a turbine that is placed in a freestream velocity of  $U_o$  from ref. [6], given by

$$P = \frac{1}{2} A \frac{u_3(u_4 + u_3)(u_4^2 - u_3^2)}{u_4 + 2u_3 - U_o} \quad (2)$$

where  $u_3$  is the velocity in the wake region and  $u_4$  is the accelerated flow velocity in the gap between the turbine and the channel walls. The values of  $u_3$  and  $u_4$  were taken from the results of the present work. It is found that the power for case 2 increases about 2.3 times compared to case 1, which is considerably less than the power increase obtained from our numerical work. The theory of ref. [6] estimates the amount of power that can be extracted from the flow; however, only a part of that power may be productive in rotating the turbine. The internal losses for case 1 may be higher compared to case 2.

## 7. Conclusions

CFD analysis of a cross-flow tidal current turbine equipped with an augmentation channel was carried out to study the effect of utilizing a larger channel area on the flow characteristics, the power output and the Coefficient of power. It was found that when a larger area of the channel is utilized, the flow velocity through the turbine increases as less of the flow bypasses the turbine system and flows through the gap between the turbine and the channel or between two turbines. In the present study, the flow velocity through the turbine and augmentation channel and the rotor almost doubled when the case of multiple equally-spaced turbines was simulated by placing solid walls with no-slip boundary conditions around the turbine and augmentation channel set-up at a distance of a quarter of the augmentation channel inlet width and height. The maximum power output increased from nearly 54 kW to slightly above 300 kW as a result. The Coefficient

of power also increased by more than 5 times for this case.

## References

- [1] Charlier RH. A “ Sleeper” awakes: tidal current power. *Renewable and sustainable energy reviews* 2003;7:187-213.
- [2] Gorban AN, Gorlov AM, Silantyev VM. Limits of the turbine efficiency for free fluid flow. *Journal of the Energy Resources Technology* 2001;123:311-7.
- [3] Garrett C, Cummins, P. Generating power from tidal currents, *ASCE Journal of Waterway, Port, Coastal and Ocean Engineering* 2004;130:114-8.
- [4] Atwater JF, Lawrence GA. Limitations of tidal power generation in a channel, *Proceedings of the 10<sup>th</sup> World Renewable Energy Congress, Glasgow, Scotland; 2008.* p. 947-52.
- [5] Bryden, IG, Couch SJ. How much energy can be extracted from moving water with a free surface: A question of importance in the field of tidal current energy. *Renewable Energy* 2007; 32:1961-6.
- [6] Garrett C, Cummins, P. The efficiency of a turbine in a tidal channel. *Journal of Fluid Mechanics* 2007; 588: 243-51.
- [7] Sutherland G, Foreman M, Garrett C. Tidal current energy assessment for Johnstone strait, Vancouver island, *Journal of Power and Energy* 2007; 221:147-57.
- [8] Blunden LS, Bahaj AS. Tidal energy resource assessment for tidal stream generators. *Journal of Power and Energy* 2007;221:137-146.
- [9] Sun X, Chick JP, Bryden IG. Laboratory-scale simulation of energy extraction from tidal currents. *Renewable Energy* 2008; 33:1267-74.
- [10] Kirke B. Developments in ducted water current turbines. Sustainable Energy Centre, University of South Australia, available online at [www.cyberiad.net/library/pdf/bk\\_tidal\\_paper25apr06.pdf](http://www.cyberiad.net/library/pdf/bk_tidal_paper25apr06.pdf)
- [11] Bahaj AS, Molland AF, Chaplin JR, Batten WMJ. Power and thrust measurements of marine current turbines under various hydrodynamic flow conditions in a cavitation tunnel and a towing tank. *Renewable Energy* 2007; 32:407-26.
- [12] Coiro DP, Maisto U, Scherillo F, Melone S, Grasso, F. Horizontal axis tidal current turbine: numerical and experimental investigations, *Proceedings of Owemes, Civitavecchia, Italy; 2006.*
- [13] Reddy H, Seshadri V, Kothari DP. Effect of draft tube size on the performance of a cross-flow turbine. *Energy Sources* 1996;18:143-149.

- [14] Prasad D, Zullah MA, Ahmed MR, Lee YH. Effect of front guide nozzle shape on the flow characteristics in an augmentation channel of a direct drive turbine for wave power generation. *Science China - Technological Sciences* 2010;53:46–51.
- [15] Olgun H. Investigation of the performance of a cross flow turbine. *International Journal of Energy Research* 1998;22:953–64.
- [16] Choi YD, Kim CG, Lee YH. Effect of wave conditions on the performance and internal flow of a direct drive turbine. *Journal of Mechanical Science and Technology* 2009;23:1693-1701.
- [17] Choi YD, Kim CG, Kim YT, Song JI, Lee YH. A performance study on a direct drive hydro turbine for wave energy converter. *Journal of Mechanical Science and Technology* 2010; 24:2197-206.
- [18] Kim KP, Ahmed MR, Hwang, YH and Lee YH. Conceptual design of a 100 kW energy-integrated type bi-directional tidal current turbine. In: *Proceedings of the 10<sup>th</sup> Asian International Conference on Fluid Machinery*. Kuala Lumpur, Malaysia; 2009, Paper 212.
- [19] [www.3ds.com/products/catia](http://www.3ds.com/products/catia)
- [20] Choi YD, Cho YJ, Kim YT, Lee YH. Performance and internal flow of a cross-flow type turbine for wave power generation. *Journal of Fluid Machinery* 2008;11:22-9.
- [21] Anderson, J. D. Jr. *Fundamentals of Aerodynamics*. 3<sup>rd</sup> ed. New York: McGraw Hill; 2001.

### **List of Tables:**

Table 1. Geometric details of cross-flow turbine and augmentation channel

### **List of Figures:**

Fig. 1. Schematic diagram of the rotor and the augmentation channel.

Fig. 2. A three-dimensional view of the augmentation channel.

Fig. 3. A three-dimensional view of the rotor blades.

Fig. 4. The meshed augmentation channel.

Fig. 5. The meshed rotor.

Fig. 6. Schematic diagram of the water channel with the set-up.

Fig. 7. Velocity vectors showing the flow of water through the augmentation channel and the rotor for case 1.

Fig. 8. Velocity vectors showing the flow of water through the augmentation channel and the rotor for case 2.

Fig. 9. Inlet velocities at augmentation channel inlet and turbine inlet at different tip speed ratios for the two cases.

Fig. 10. Velocity vectors showing the flow of water through the rotor.

Fig. 11. Iso-pressure contours in the main flow domain.

Fig. 12. Power output of the turbine for the two cases.

Fig. 13. Coefficient of power for the two cases.



Table 1: Geometric details of cross-flow turbine and augmentation channel

Number of blades	26
Blade angle at outer periphery	30°
Blade angle at inner periphery	90°
Axial length of blade	8,700 mm
External diameter	6,050 mm
Internal diameter	3,850 mm
Clearance of turbine & housing	20.6 mm
Length of blade	1,119.6 mm
Thickness of blade	66 mm
Total length of augmentation channel ( $2 \times H1$ )	17.4 m
Cross-section of augmentation channel at inlet ( $V1 \times$ width)	8.7 m $\times$ 8.7 m
Cross-section of augmentation channel at outlet	8.7 m $\times$ 4.35 m

Figure 1

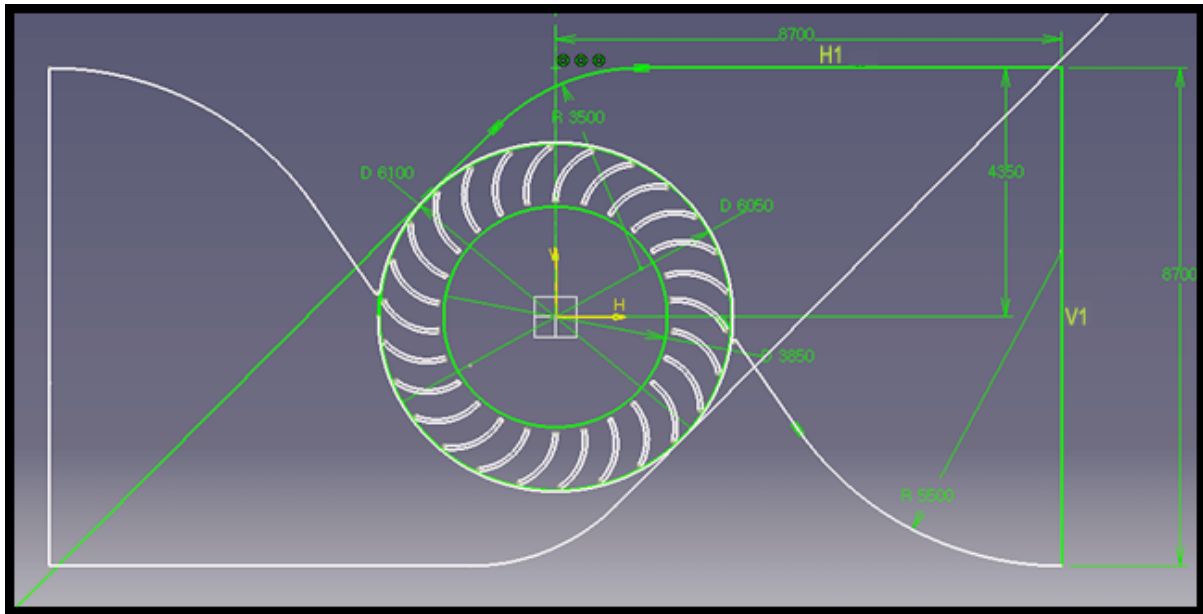


Fig. 1. Schematic diagram of the rotor and the augmentation channel.

Figure 2

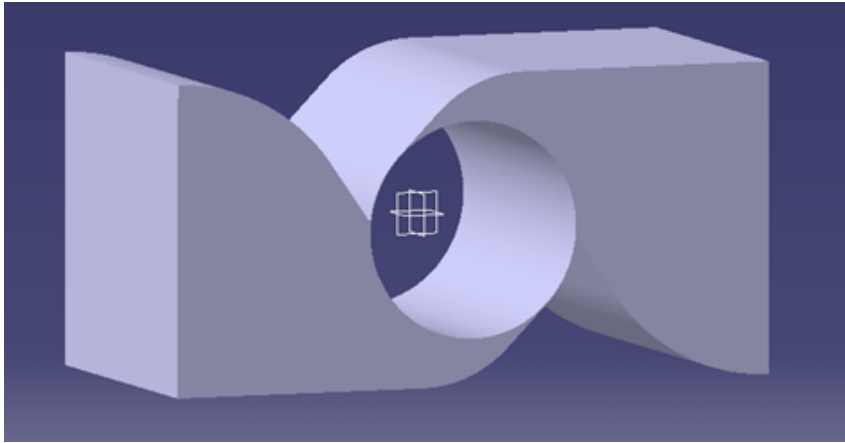


Fig. 2. A three-dimensional view of the augmentation channel.

Figure 3

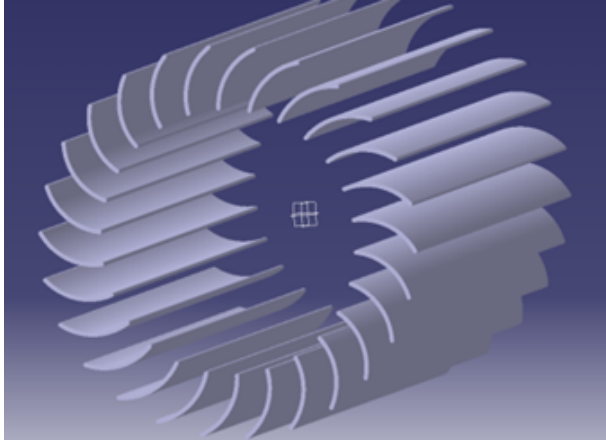


Fig. 3. A three-dimensional view of the rotor blades.

Figure 4

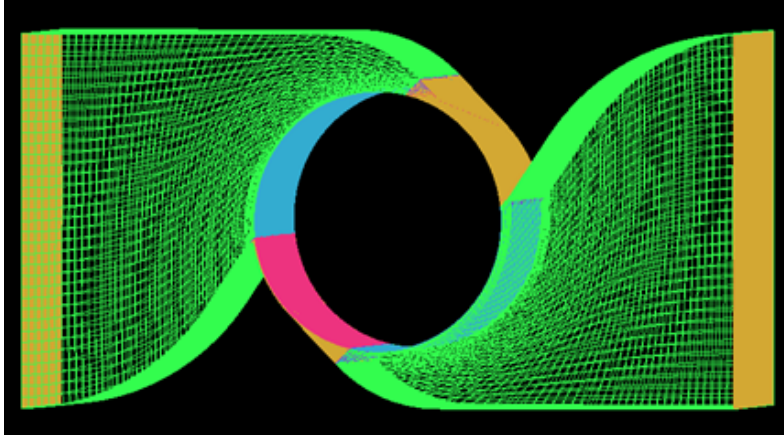


Fig. 4. The meshed augmentation channel.

Figure 5

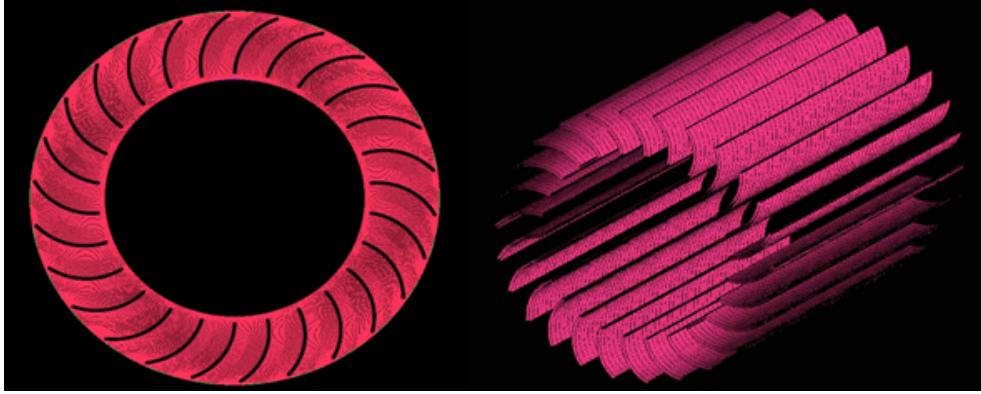


Fig. 5. The meshed rotor.

Figure 6

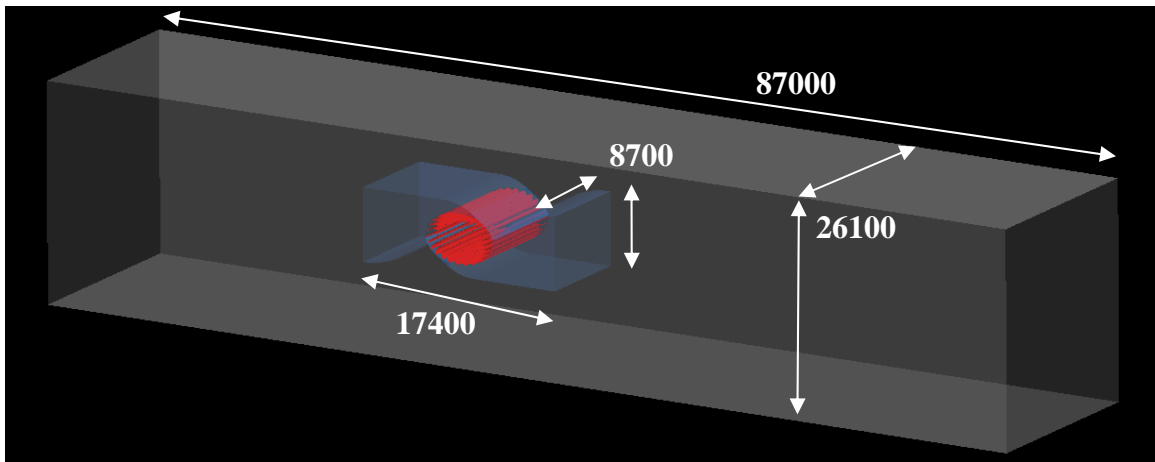


Fig. 6. Schematic diagram of the water channel with the set-up (all dimensions are in mm).

Figure 7

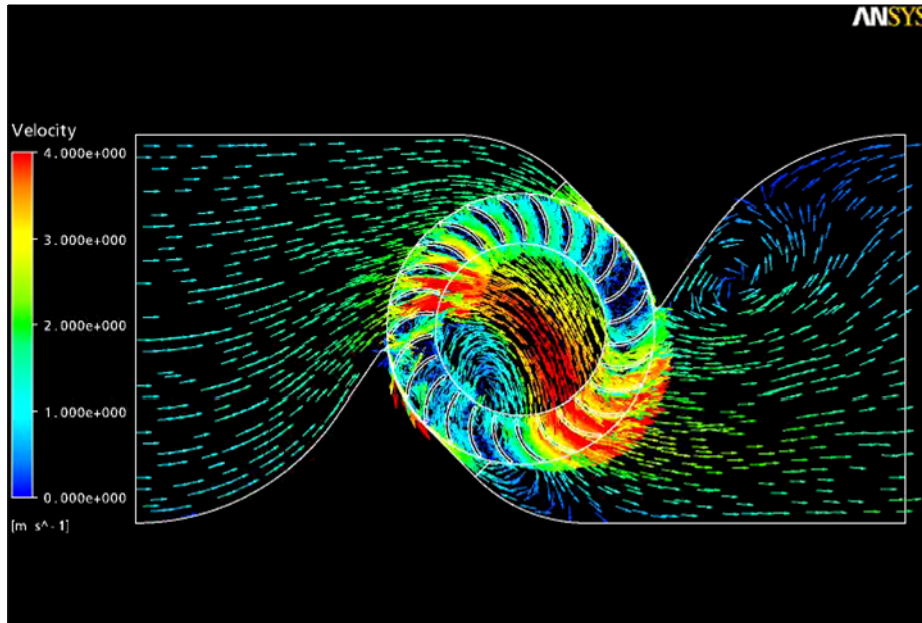


Fig. 7. Velocity vectors showing the flow of water through the augmentation channel and the rotor for case 1.



Figure 8

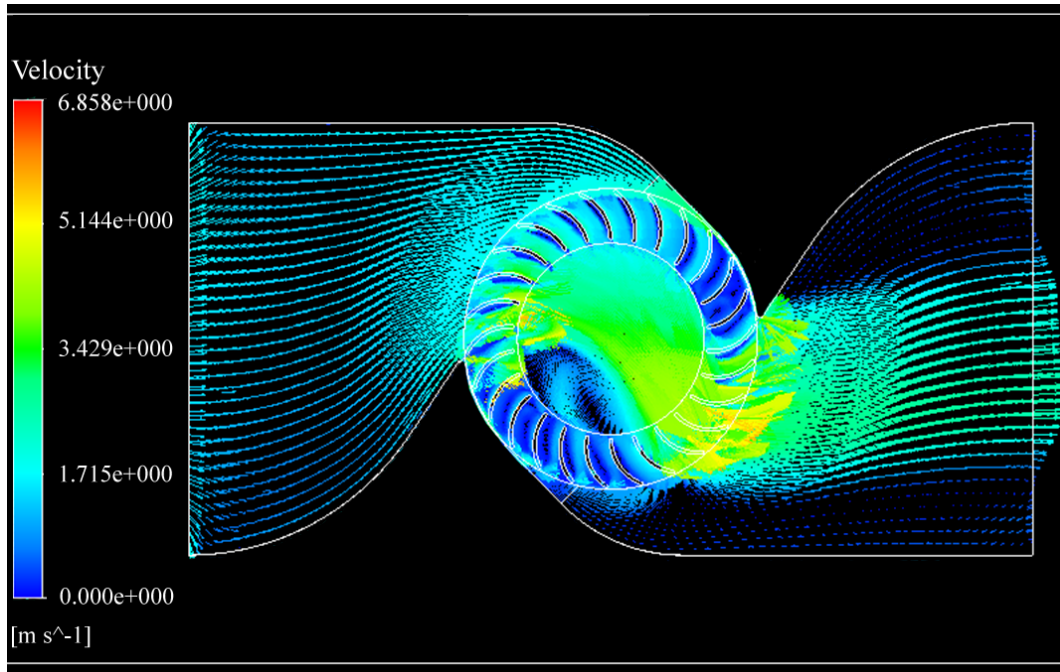


Fig. 8. Velocity vectors showing the flow of water through the augmentation channel and the rotor for case 2.

Figure 9

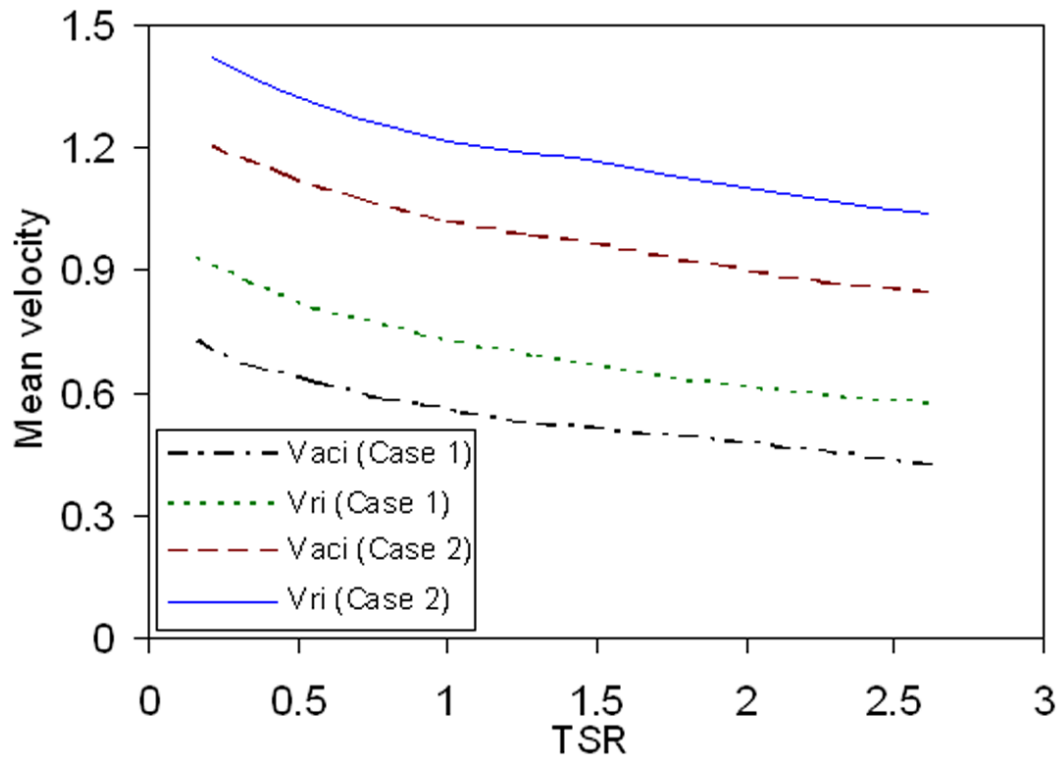


Fig. 9. Inlet velocities at augmentation channel inlet and turbine inlet at different tip speed ratios for the two cases.

Figure 10

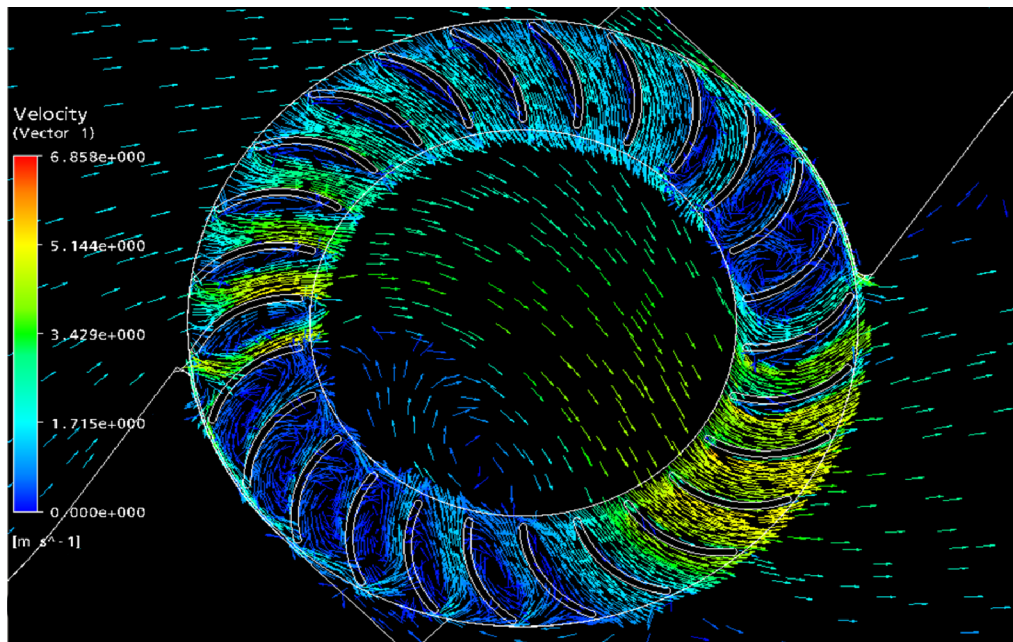


Fig. 10. Velocity vectors showing the flow of water through the rotor.

Figure 11

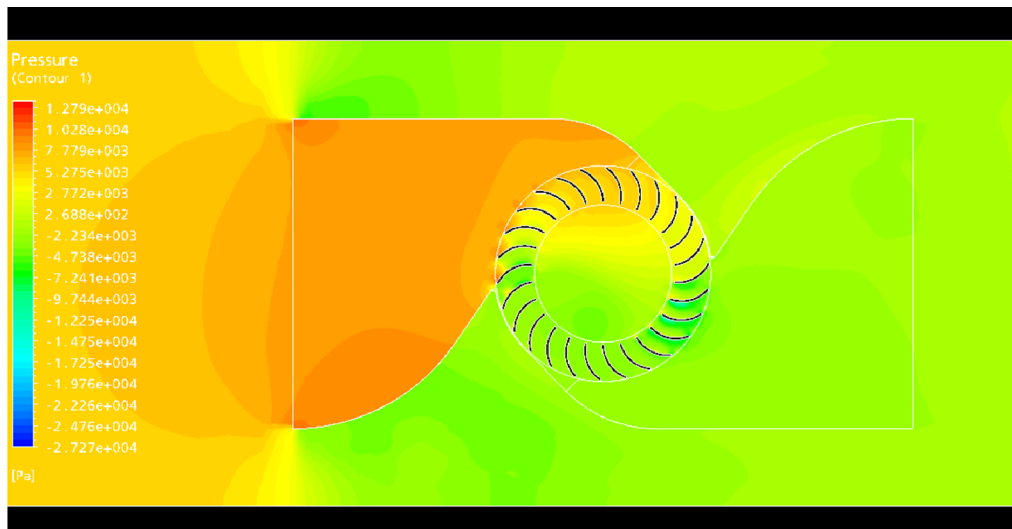


Fig. 11. Iso-pressure contours in the main flow domain.

Figure 12

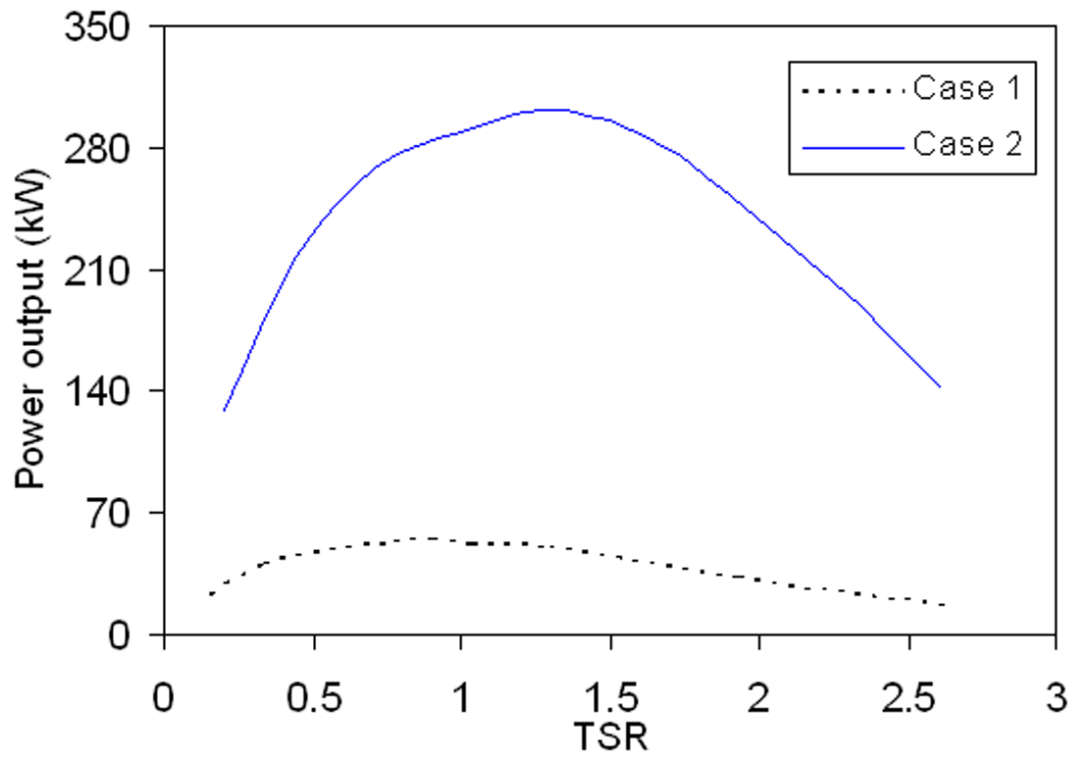


Fig. 12. Power output of the turbine for the two cases.

Figure 13

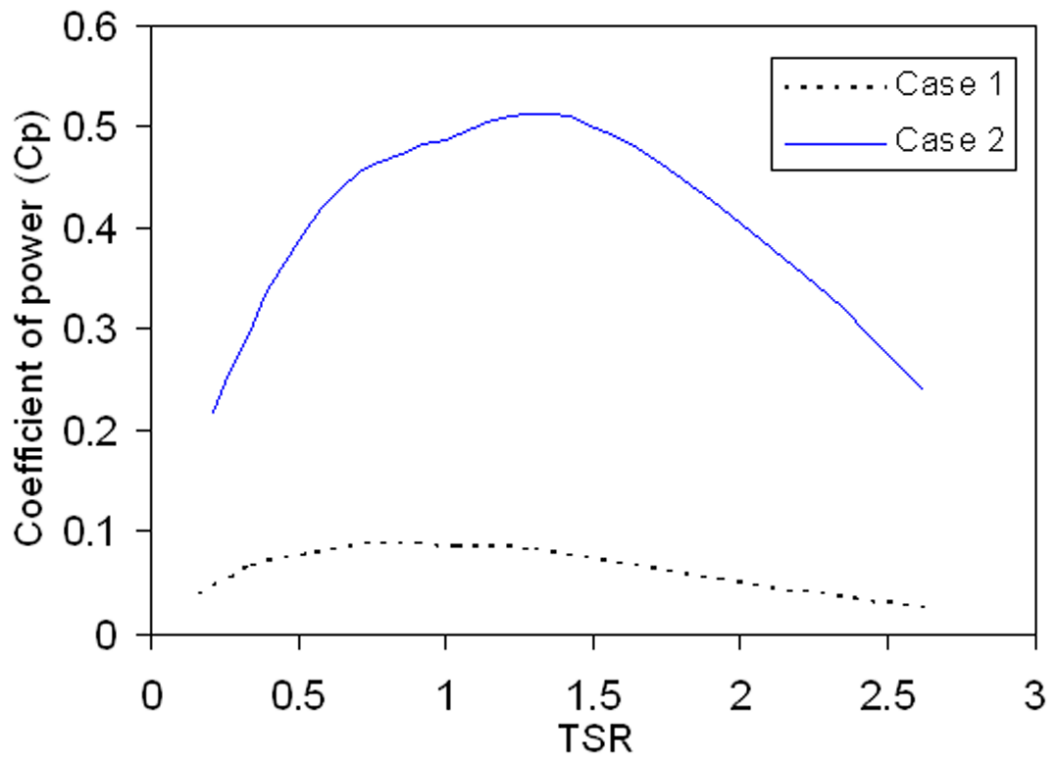


Fig. 13. Coefficient of power for the two cases.